Blackburn, P., Wilson, G., & Moore, S. (1977) *J. Biol. Chem. 252*, 5904-5910.
Burton, L. E., Blackburn, P., & Moore, S. (1980) *Int. J. Pept. Protein Res. 16*, 359-364.
Fett, J. W., Strydom, D. J., Lobb, R. R., Alderman, E. M., Bethune, J. L., Riordan, J. F., & Vallee, B. L. (1985) *Biochemistry 24*, 5480-5486.
Henderson, P. J. F. (1972) *Biochem. J. 127*, 321-333.
Lee, F. S., Auld, D. S., & Vallee, B. L. (1989) *Biochemistry* (preceding paper in this issue).
Morrison, J. F. (1969) *Biochim. Biophys. Acta 185*, 269-286.
Shapiro, R., & Vallee, B. L. (1987) *Proc. Natl. Acad. Sci. U.S.A. 84*, 2238-2241.
Shapiro, R., Riordan, J. F., & Vallee, B. L. (1986a) *Biochemistry 25*, 3527-3532.
Shapiro, R., Fett, J. W., Strydom, D. J., & Vallee, B. L. (1986b) *Biochemistry 25*, 7255-7264.
Strydom, D. J., Fett, J. W., Lobb, R. R., Alderman, E. M., Bethune, J. L., Riordan, J. F., & Vallee, B. L. (1985) *Biochemistry 24*, 5486-5494.
Turner, P. M., Lerea, K. M., & Kull, F. J. (1983) *Biochem. Biophys. Res. Commun. 114*, 1154-1160.
Witzel, H. (1963) *Prog. Nucleic Acid Res. Mol. Biol. 2*, 221-258.
Witzel, H., & Barnard, E. A. (1962) *Biochem. Biophys. Res. Commun. 7*, 295-299.

Concerted Two-Dimensional NMR Approaches to Hydrogen-1, Carbon-13, and Nitrogen-15 Resonance Assignments in Proteins†

Brian J. Stockman, Michael D. Reily,‡ William M. Westler, Eldon L. Ulrich, and John L. Markley*

Department of Biochemistry, College of Agricultural and Life Sciences, 420 Henry Mall, University of Wisconsin—Madison, Madison, Wisconsin 53706

Received June 7, 1988; Revised Manuscript Received August 21, 1988

ABSTRACT: When used in concert, one-bond carbon–carbon correlations, one-bond and multiple-bond proton–carbon correlations, and multiple-bond proton–nitrogen correlations, derived from two-dimensional (2D) NMR spectra of isotopically enriched proteins, provide a reliable method of assigning proton, carbon, and nitrogen resonances. In contrast to procedures that simply extend proton assignments to carbon or nitrogen resonances, this technique assigns proton, carbon, and nitrogen resonances coordinately on the basis of their integrated coupling networks. Redundant spin coupling pathways provide ways of resolving overlaps frequently encountered in homonuclear ^{1}H 2D NMR spectra and facilitate the elucidation of complex proton spin systems. Carbon–carbon and proton–carbon couplings can be used to bridge the aromatic and aliphatic parts of proton spin systems; this avoids possible ambiguities that may result from the use of nuclear Overhauser effects to assign aromatic amino acid signals. The technique is illustrated for *Anabaena* 7120 flavodoxin and cytochrome *c*-553, both uniformly enriched with carbon-13 (26%) or nitrogen-15 (98%).

Nuclear magnetic resonance is the only serious competitor to X-ray crystallography for detailed structural studies of proteins. NMR[1] structures determined in solution are of low resolution, but they may better represent the physiological conformations or the dynamic properties of proteins than structures derived from crystals. In addition, NMR can be used to investigate conformational equilibria, interactions of proteins with other proteins or small molecules, and reaction pathways involving covalent protein modification.

The key step in protein NMR investigations is the assignment of proton, carbon, and nitrogen resonances to specific amino acids in the protein. The most successful approach in small proteins has been to first assign the proton spin systems by using a combination of two-dimensional (2D) homonuclear proton NMR experiments (Billeter, 1982; Wüthrich et al., 1982; Wüthrich, 1986), such as COSY (Nagayama et al., 1980), NOESY (Kumar et al., 1980), RELAY (Bax & Drobny, 1985), and HOHAHA (Davis & Bax, 1985). Proton assignments are then extended to carbon or nitrogen resonances by using heteronuclear correlation experiments (Chan & Markley, 1982; Kojiro & Markley, 1983; Ortiz-Polo et al., 1986; Glushka & Cowburn, 1987; Sklenar & Bax, 1987). The complexity and overlaps in homonuclear ^{1}H{^{1}H} 2D spectra, however, make this approach difficult with larger proteins (M_r >10 000).

Heteronuclei can be used to resolve overlaps in 2D proton spectra. Examples include spectral editing techniques for

† Supported by USDA Competitive Research Grant 85-CRCR-1-1589 and NIH Grant RR02301. This study made use of the National Magnetic Resonance Facility at Madison, which is supported in part by NIH Grant RR02301 from the Biomedical Research Technology Program, Division of Research Resources. Equipment in the facility was purchased with funds from the University of Wisconsin, the NSF Biological Biomedical Research Technology Program (Grant DMB-8415048), the NIH Shared Instrumentation Program (Grant RR02781), and the U.S. Department of Agriculture. B.J.S. is supported by an NIH Training Grant in Cellular and Molecular Biology (GM07215).

* To whom correspondence should be addressed.
‡ Present address: Park Davis, Research Division, Warner Lambert Co., 2800 Plymouth Rd., Ann Arbor, MI 48105.

[1] Abbreviations: 2D, two dimensional; COSY, correlated spectroscopy; DQC, double quantum correlation; HOHAHA, homonuclear Hartmann-Hahn; INADEQUATE, incredible natural abundance double quantum transfer; MBC, multiple-bond correlation; NMR, nuclear magnetic resonance; NOESY, nuclear Overhauser spectroscopy; RELAY, relayed correlated spectroscopy; SBC, single-bond correlation; TMS, tetramethylsilane; TSP, (trimethylsilyl)propionic acid.

0006-2960/89/0428-0230$01.50/0

observing nuclear Overhauser effects to or from protons bound to selectively enriched nuclei (Griffey et al., 1985; Griffey & Redfield, 1987; Rance et al., 1987; McIntosh et al., 1987; Senn et al., 1987) and $^1H\{^{13}C\}$RELAY experiments (Brühwiler & Wagner, 1986). Proton, carbon, or nitrogen assignments made with these techniques, however, are limited to correlations with resonances previously assigned.

The procedure presented here enables the concerted assignment of proton, carbon, and nitrogen resonances in proteins. The technique relies on a combination of one-bond ^{13}C–^{13}C, one-bond ^1H–^{13}C, multiple-bond ^1H–^{13}C, and multiple-bond ^1H–^{15}N correlations. Coupling constant magnitudes for these correlations observed in peptides are as follows (Bystrov, 1976): $^1J_{CH}$, 120–170 Hz; $^2J_{CH}$, 2–8 Hz; $^3J_{CH}$, 0–7 Hz; $^1J_{CC}$, 35–65 Hz; $^2J_{NH}$, 0–2 Hz; $^3J_{NH}$, 0–4 Hz. The angular dependence of $^3J_{CH}$ and $^3J_{NH}$ (and to a lesser extent $^2J_{CH}$ and $^2J_{NH}$) can be correlated with molecular structure (Karplus & Karplus, 1972; Bystrov, 1976). ^{13}C correlations are obtained from $^{13}C\{^{13}C\}$DQC spectra (Oh et al., 1988; Stockman et al., 1988b; Westler et al., 1988a). ^1H–^{13}C correlations are obtained from $^1H\{^{13}C\}$SBC spectra (Bax et al., 1983). Multiple-bond ^1H–^{13}C and ^1H–^{15}N correlations are obtained from $^1H\{^{13}C\}$MBC and $^1H\{^{15}N\}$MBC spectra (Bax & Summers, 1986). The full information content of these four types of spectra is realized only when they are analyzed simultaneously. Each complements the others by resolving spectral overlap or by adding redundancy to well-resolved regions, thereby increasing the reliability of the assignments. The technique is demonstrated for two cyanobacterial proteins, oxidized flavodoxin (M_r 21 000) and reduced cytochrome *c*-553 (M_r 11 000) from *Anabaena* 7120.

Materials and Methods

Protein Enrichment and Purification. The proteins studied were enriched uniformly with ^{13}C (26%) or ^{15}N (98%). With proteins, carbon-13 enrichment at a level of 20–30 atom % is required for the $^{13}C\{^{13}C\}$DQC experiment, since low concentrations must be used and the occurrence of adjacent carbon-13 atoms at natural abundance is only 0.012%. *Anabaena* 7120 was grown as described previously (Stockman et al., 1988a). To obtain protein uniformly enriched with ^{15}N, $K^{15}NO_3$ (98+ atom % isotopic purity) was used as the sole nitrogen source. Protein enriched uniformly with ^{13}C was obtained by supplying $^{13}CO_2$ (26 atom % isotopic purity) as the sole carbon source. Flavodoxin was purified by the procedure of D. W. Krogmann (personal communication). Protein fractions with A_{466}/A_{276} ratio greater than 0.14 were considered to be pure. Cytochrome *c*-553 was purified according to Ulrich (1978). Cytochrome *c*-553 samples were reduced by adding an excess of dithionite just prior to NMR measurements. Air above the sample was replaced with argon to prevent oxidation during NMR experiments.

Chemicals. $K^{15}NO_3$ (98+ atom %) was purchased from the Mound Facility of the Monsanto Research Corp. $^{13}CO_2$ (99+ atom %) was purchased from Isotec, Inc. The $^{13}CO_2$ was diluted with natural abundance CO_2 to 26 atom % isotopic purity (as measured by ^{13}C satellite intensities in the ^1H NMR spectra of individual amino acids) and mixed with air to 10% CO_2. Other chemicals were of reagent grade or better.

NMR Spectroscopy. All spectra were obtained on a Bruker AM-500 (11.7 T) spectrometer. Proton chemical shifts are referenced to internal TSP. Experimental carbon chemical shifts were determined relative to external dioxane, which was assigned a chemical shift of 67.8 ppm relative to TMS. Experimental nitrogen chemical shifts were determined relative to external ammonium sulfate, which was assigned a chemical shift of 22.3 ppm relative to liquid ammonia.

$^{13}C\{^{13}C\}$DQC spectra (125.77 MHz) were collected with a Bruker 5-mm broad-band probe and a ^{13}C-selective preamplifier. The pulse sequence used was a modification (Westler et al., 1988a) of the resonance-offset-compensated INADEQUATE experiment (Levitt & Ernst 1983). WALTZ-16 (Shaka et al., 1983) composite pulse decoupling was used during acquisition to decouple attached protons.

The $^1H\{^{13}C\}$SBC, $^1H\{^{13}C\}$MBC, and $^1H\{^{15}N\}$MBC spectra were collected with a Bruker 5-mm inverse broad-band probe, using Bruker reverse electronics. Protons were pulsed with the decoupler, while the other nuclei were pulsed with the transmitter. The pulse sequence used for the $^1H\{^{13}C\}$SBC experiments was that of Bax et al. (1983). WALTZ-16 decoupling at the carbon frequency was used during acquisition to collapse proton–carbon couplings. The $^1H\{^{13}C\}$MBC and $^1H\{^{15}N\}$MBC experiments used the pulse sequence of Bax and Summers (1986). See the figure legends for additional experimental parameters.

Results

Aliphatic Side Chains. Comparisons of spectral regions illustrate how the information content of one type of spectrum can be used to sort out or confirm information available in the other types of spectra. Figure 1 shows corresponding aliphatic regions of the $^{13}C\{^{13}C\}$DQC and $^1H\{^{13}C\}$MBC spectra of flavodoxin. The carbon dimension (vertical axis) is identical in each spectrum. In Figure 1A, each pair of coupled carbon atoms is represented by a pair of antiphase doublets located at their double-quantum frequency on the horizontal axis; each individual antiphase doublet is located at its single-quantum frequency on the vertical axis. Vertical lines in this spectrum connect resonances from single-bond coupled carbon atoms. Many amino acid carbon spin systems can be identified easily by their characteristic connectivity patterns (Oh et al., 1988; Stockman et al., 1988b).

Some regions of the $^{13}C\{^{13}C\}$DQC spectrum, however, are very crowded. This overlap can be resolved by spreading the carbon chemical shifts out in the proton dimension by means of the $^1H\{^{13}C\}$MBC (Figure 1B) and $^1H\{^{13}C\}$SBC (Figure 2) coupling patterns characteristic for a given amino acid. The use of information from one spectrum to analyze another is exemplified by the outlined leucine connectivities. In Figure 1A, the leucine $^{13}C\{^{13}C\}$DQC correlations are not resolved. In Figure 1B, however, long-range proton–carbon coupling patterns characteristic of the pairs of leucine δ-methyl protons are observed. These connectivities assign the β-, γ-, δ_1-, and δ_2-carbon resonances in the $^{13}C\{^{13}C\}$DQC spectrum (Figure 1A). The positions of the δ_1- and δ_2-carbon and δ_1- and δ_2-proton resonances are confirmed in Figure 2, which shows the $^1H\{^{13}C\}$SBC correlations for these and other methyl groups.

The outlined alanine, threonine, and valine spin systems illustrate how redundant connectivities can be obtained from information in each type of 2D spectrum. Each carbon spin system is resolved in Figure 1A. The long-range coupling patterns of the methyl protons seen in Figure 1B confirm the carbon spin system assignments as well as assign the methyl proton chemical shifts. The methyl proton and carbon chemical shifts are also verified in Figure 2.

The carbonyl carbon region of the $^1H\{^{13}C\}$MBC spectrum (Figure 3A) and the amide nitrogen region of the $^1H\{^{15}N\}$MBC spectrum (Figure 3B) of flavodoxin show several correlations with alanine α- or β-protons. These spectra allow the extension of side-chain assignments to the main-chain carbonyl carbon and amide nitrogen resonances. Representative aliphatic proton and carbon spin system assignments in flavodoxin and

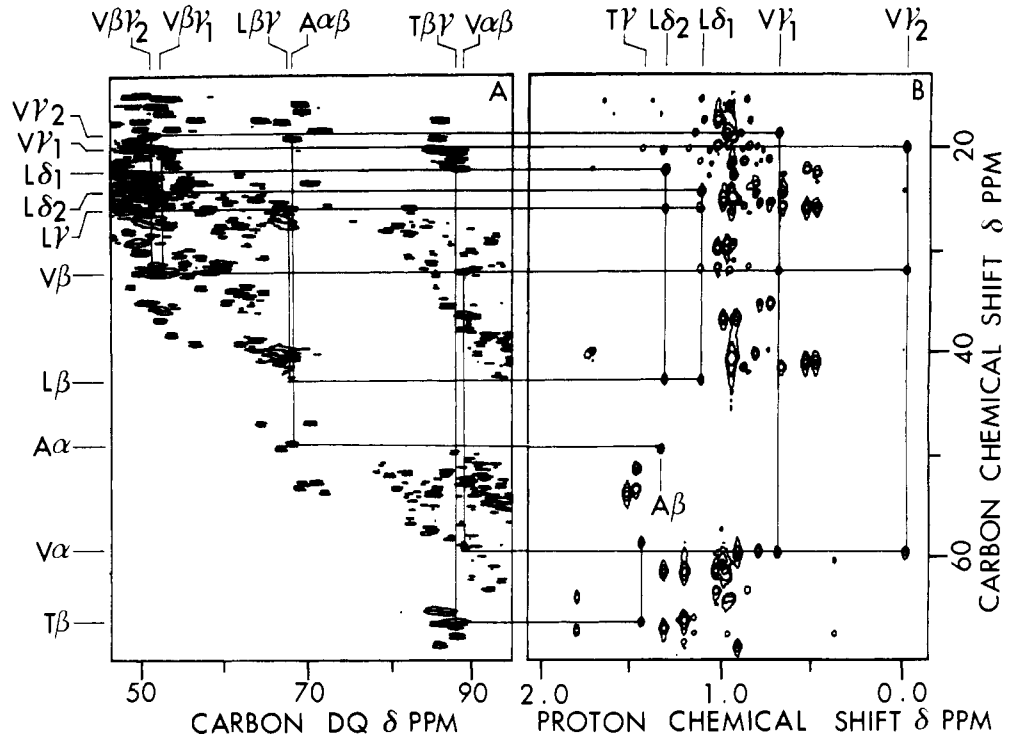

FIGURE 1: Composite 11.7-T NMR spectra of flavodoxin showing a portion of the aliphatic proton and carbon region. The same region of the carbon spectrum (vertical axis) is shown in both contour plots. The sample was 7 mM [^{13}C]flavodoxin (26% uniformly labeled) in ^2H_2O containing 150 mM phosphate buffer at pH 7.5; the total sample volume was 0.4 mL in a 5-mm (o.d.) NMR tube. Labeled positions along the horizontal and vertical axes identify cross peaks located at their intersection. The notation used in the labels is *Pr*, where *P* is the single-letter amino acid abbreviation and *r* is the Greek letter(s) identifying the atom(s) involved in the correlation. Only selected spin systems are outlined in the figure; they correspond to the first spin system of each type of amino acid listed in Table I. (A) A small region of the ^{13}C{^{13}C}DQC spectrum. The total experiment time (96 h) consisted of 512 blocks each containing the average of 384 free induction decays (8192 data points each). The 90° carbon pulse was 6.6 μs. The sweep width was 22 727 Hz. The total delay for the double-quantum propagator was set to 9.1 ms. The acquisition time was 0.18 s with a relaxation delay of 1.5 s. The single-quantum frequency is plotted along the vertical axis, and the double-quantum frequency is plotted along the horizontal axis. (B) A region of the ^{1}H{^{13}C}MBC spectrum. A total of 512 blocks containing the average of 104 free induction decays (4096 data points each) were collected. The 90° proton pulse was 9.3 μs; the 90° carbon pulse was 11 μs. The proton sweep width was 7246 Hz, and the carbon sweep width was 22 727 Hz. The delay time used to suppress one-bond correlations was 3.57 ms. The delay time used to optimize for 7-Hz carbon–proton couplings was 70 ms. The acquisition time was 0.283 s with a relaxation delay of 1.8 s.

cytochrome *c*-553 obtained from these data are presented in Table I.

Aromatic Side Chains. The aromatic portions of the proton and carbon spin systems for each of the six aromatic side chains in cytochrome *c*-553 and most of the aromatic residues in flavodoxin have been elucidated. Figure 4A illustrates the one-bond carbon–carbon correlations observed in the ^{13}C-{^{13}C}DQC spectrum for the β-carbons and aromatic carbons of the single tryptophan, one of the two tyrosine, and one of the two phenylalanine residues, along with the one-bond carbon–carbon correlations observed for the β-, γ-, and δ_1-carbons of the iron-ligated histidine residue in cytochrome *c*-553. The characteristic ^{13}C{^{13}C}DQC connectivity patterns (Oh et al., 1988) allow easy identification of each carbon resonance. The tryptophan carbon chemical shifts in both flavodoxin and cytochrome *c*-553 are in general agreement with those observed in model peptides.[2]

Extension of the carbon assignments obtained from the ^{13}C{^{13}C}DQC data to the corresponding β-protons (Figure 4B) and aromatic ring protons (Figure 5A) was accomplished by using ^{1}H{^{13}C}SBC data. Many of the carbon and proton resonance assignments were verified by cross peaks in the ^{1}H{^{13}C}MBC spectrum (Figure 5B); characteristic long-range coupling patterns were observed for several types of aromatic protons. Note that redundancy in the ^{1}H and ^{13}C chemical shifts for the pair of symmetric δ- or ε-atoms of the phenylalanine and tyrosine rings (presumably from ring flips that are rapid on the NMR time scale) results in identical cross peaks for the δ or ε correlations in ^{1}H{^{13}C}SBC and ^{1}H{^{13}C}-MBC spectra.

Figure 6 illustrates how ^{1}H{^{15}N}MBC data were used to assign the aromatic nitrogen resonances in flavodoxin. The tryptophan ϵ_1-nitrogen assignments were based on proton assignments made according to the method outlined in Figures 4 and 5. Tryptophan ϵ_1-nitrogens are difficult to assign by other methods because they resonate near the amide backbone region (100–135 ppm), but since no other cross peaks occur in this region of the ^{1}H{^{15}N}MBC spectrum, the assignments here are unambiguous. Histidine δ_2- and ϵ_1-proton correlations to both of the δ_1- and ϵ_2-nitrogens are observed as a characteristic box-shaped pattern. ^{1}H{^{15}N}MBC presents an alternative to ^{15}N decoupling (Smith et al., 1987) for indentifying histidine δ_2- and ϵ_1-proton and tryptophan δ_1-proton resonances in ^{15}N-enriched proteins. Table II summarizes the aromatic amino acid proton, carbon, and nitrogen chemical shifts in flavodoxin and cytochrome *c*-553.

DISCUSSION

The experiments outlined above demonstrate the usefulness of 2D homonuclear ^{13}C and 2D heteronuclear NMR in sim-

[2] The tryptophan η_2- and ζ_3-carbon chemical shifts in *Anabaena* 7120 flavodoxin and cytochrome *c*-553 are reversed with respect to the chemical shifts reported by Richarz and Wüthrich (1978). A reinvestigation of the tryptophan ^{13}C spectrum using a model peptide (K-W-K) indicated that the η_2- and ζ_3-carbon assignments of Richarz and Wüthrich should be reversed (B. H. Oh and J. L. Markley, unpublished experiments).

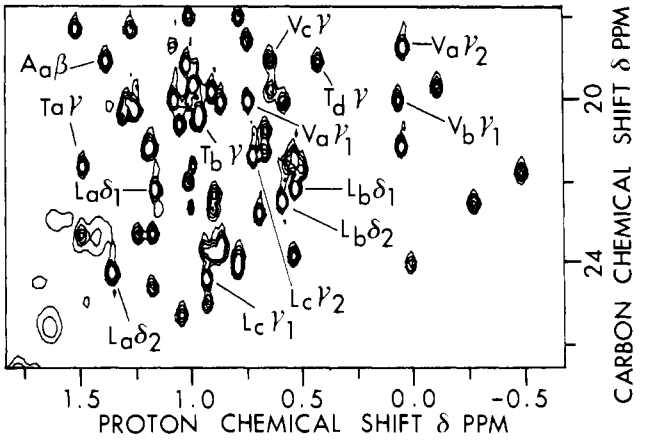

FIGURE 2: Methyl region of the 11.7-T NMR $^1H\{^{13}C\}$SBC spectrum of flavodoxin. The notation is P_qr, where P is the single-letter amino acid abbreviation, q corresponds to the amino acid lettering in the data tables, and r is the Greek letter identifying the carbon and proton atoms involved in the correlation. A total of 552 blocks containing the average of 72 free induction decays (2048 data points each) were collected. The 90° proton pulse was 6.7 μs; the 90° carbon pulse was 71 μs. The proton sweep width was 6944 Hz, and the carbon sweep width was 9433 Hz. The carbon sweep width covered only the aliphatic region so that higher digital resolution in the ^{13}C dimension could be obtained. The spectrum of the aromatic region was collected separately. The delay time used was 3.57 ms to optimize for 140-Hz carbon–proton couplings. The acquisition time was 0.147 s with a relaxation delay of 1.8 s.

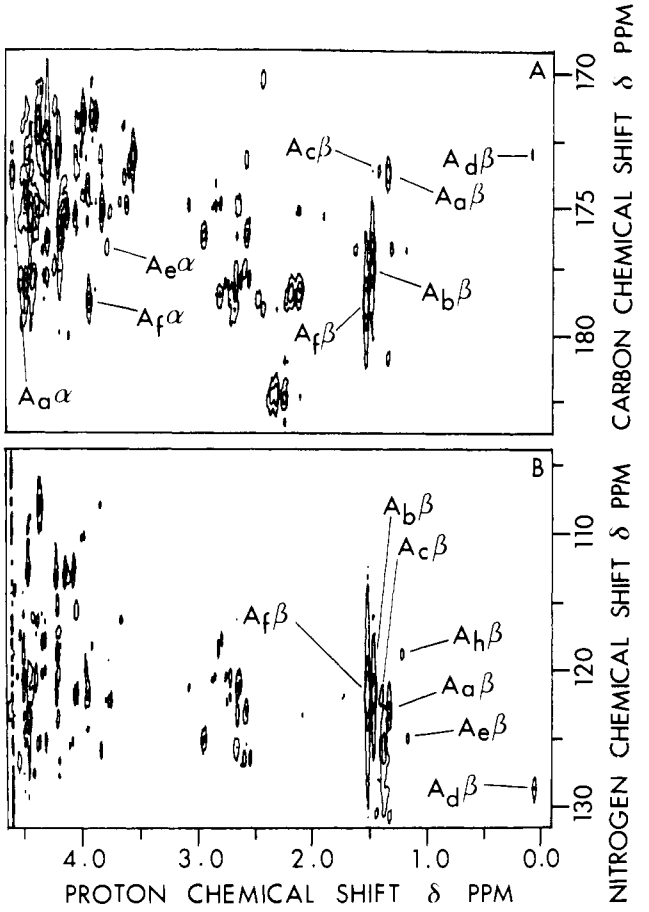

FIGURE 3: Peptide backbone spectral regions in the multiple-bond correlation NMR spectra (at 11.7 T) of flavodoxin. The proton dimension (horizontal axis) is identical in the two contour plots. Peaks are labeled as in Figure 2, except that r is the Greek letter identifying the type of proton involved in the correlation. The vertical axis corresponds to the chemical shifts of the main-chain carbonyl carbon or amide nitrogen. (A) A region of the $^1H\{^{13}C\}$MBC spectrum. Sample conditions and experimental parameters were as described in Figure 1. (B) A region of the $^1H\{^{15}N\}$MBC spectrum. The sample was 10 mM [^{15}N]flavodoxin (95% uniformly labeled) in ^2H_2O containing 150 mM phosphate buffer at pH 7.5. The sample had been preexchanged in ^2H_2O for 2 h at 65 °C to deuteriate all NH, NH_2, and NH_3 groups. The total sample volume was 0.4 mL in a 5-mm (o.d.) NMR tube. A total of 512 blocks containing the average of 80 free induction decays (4096 data points each) were collected. The 90° proton pulse was 8.2 μs; the 90° nitrogen pulse was 20 μs. The proton sweep width was 7246 Hz, and the nitrogen sweep width was 11 111 Hz. No pulse was used to suppress one-bond couplings since the sample had been preexchanged with ^2H_2O. A 70-ms delay time was used to optimize for 7-Hz couplings. The acquisition time was 0.283 s with a relaxation delay of 2.0 s.

plifying the assignment of ^1H spin systems in proteins, as well as in assigning carbon and nitrogen resonances. To date, these techniques have been used to assign complete ^1H, ^{13}C, and ^{15}N spin systems for 41 amino acid side chains in flavodoxin and for 39 amino acid side chains in cytochrome *c*-553. In addition, complete ^{13}C spin systems have been assigned for 36 side chains in flavodoxin (Stockman et al., 1988b). The increased expense of obtaining uniformly carbon-13- or nitrogen-15-labeled proteins is offset by the increased efficiency and reliability of assignments. The approach automatically provides extensive ^{13}C and ^{15}N resonance assignments in proteins, which heretofore have been unavailable. These assignments can be utilized in a number of ways.

Previous assignments of quaternary carbons required indirect techniques, such as chemical modification, relaxation probes, or the use of variant proteins (Allerhand, 1979; Chan et al., 1983). They are assigned directly by the methods described here. Specific assignments of tyrosine ζ-carbons, which frequently can be resolved in the one-dimensional ^{13}C spectrum, will be useful in investigations of tyrosine pK_a values or enzyme mechanisms thought to involve tyrosine.

This assignment strategy will facilitate ^{13}C and ^{15}N relaxation studies of protein dynamics in solution. T_1 measurements for the backbone atoms can lead to a better understanding of the local mobilities of each region of the protein (McCain et al., 1988). T_1 measurements for side-chain atoms can reflect local mobility and thus can give clues as to whether side chains are located on the surface or are buried within the protein (Jardetzky, 1981; Smith et al., 1987).

The four-bond coupling between the aliphatic β-protons and aromatic δ-protons of aromatic amino acids usually is too small, compared with the line width, for practical correlations in proteins. One exception has been the use of long-range proton–proton couplings to assign some histidine side-chain protons in a myoglobin (Dalvit et al., 1987). The usual procedure (Billeter et al., 1982) for cross assigning the aromatic and aliphatic portions of the proton spin systems of aromatic amino acids relies on the observation of NOESY cross peaks between one or two ring protons (δ in phenylalanine, tyrosine, and histidine; δ and/or ε in tryptophan) and the β-protons of the side chain. In theory, the distance in all possible ring orientations between at least one ring proton and the β-protons is short enough to result in a NOESY cross peak, except for some orientations of the histidine ring (Billeter et al., 1982). Ambiguities arise, however, when NOESY cross peaks are observed between one set of β-protons and more than one aromatic spin system, or vice versa. Specific assignments are difficult in these circumstances, because one may not be able to distinguish the desired intraresidue cross peak(s) from interresidue cross peak(s). The alternative approach presented here is based on one-bond scalar coupling. The aromatic ring carbon spin systems can be entered via their proton resonances; then, by following carbon–carbon correlations around the ring, the β-carbon can be assigned. Proton–carbon correlations to

Table I: Representative Aliphatic Amino Acid Proton, Carbon, and Nitrogen Chemical Shifts in *Anabaena* 7120 Flavodoxin and Cytochrome *c*-553

		carbon				proton				nitrogen
amino acid[a]	o	α	β	γ	δ	α	β	γ^b	δ^b	α
					Flavodoxin					
Ala-a	173.9	49.3	19.1			4.65	1.39			122.8
Ala-b	177.4	53.1	18.3			4.29	1.52			121.6
Ala-c	173.8	49.7	17.5				1.47			122.1
Ala-d	173.1	47.3	17.2			3.95	0.14			128.6
Ala-e	176.7	53.2	16.3			3.83	1.23			124.9
Ala-f	178.6	53.7	15.6			3.98	1.58			121.8
Ala-g		47.2	23.4			5.60	1.48			
Ala-h	177.6	54.2	18.3				1.27			118.7
Thr-a		58.3	66.1	21.8				1.49		
Thr-b		59.5	68.4	20.4		4.41	4.08	0.96		
Thr-c		61.1	65.9	20.3		3.89		1.25		
Thr-d		60.1	67.2	19.1		4.48		0.43		
Leu-a			42.7	26.1	22.3, 24.6				1.17, 1.37	
Leu-b			40.8	26.0	23.3, 23.6				0.53, 0.59	
Leu-c			41.5	25.8	24.6, 21.5				0.94, 0.73	
Val-a		59.4	32.1	20.2, 18.9		4.10		0.74, 0.05		
Val-b		62.7	28.3	20.1, 15.5				0.07, −0.14		
Val-c		60.9	30.2	19.1, 19.1				0.65, 0.65		
Val-d		65.2	28.6	22.4, 17.5				0.89, −0.19		
					Cytochrome *c*-553					
Ala-a	175.2	49.7	17.4			4.44	1.29			118.8
Ala-b	177.3	52.3	16.2			3.88	1.58			117.1
Ala-c	177.4	54.6	15.5			3.91	1.39			125.9
Gly-a	171.4	44.2				3.71				
Gly-b	175.8	45.1				3.73				
Gly-c	174.4	45.8				4.09, 4.14				
Ser-a	174.3	59.9	61.4			4.19				
Ser-b	174.1	60.2	61.2			3.72	4.09			
Thr-a	172.4	60.6	67.1	19.3		3.50	4.52	1.11		
Thr-b	172.9	66.7	67.5	19.4		3.32	4.05	1.05		

[a] Since the primary sequence has not been determined for either of these proteins, amino acids of a given type have been assigned a letter here and in the figures. [b] Leucine δ-proton and valine γ-proton chemical shifts are listed in the same order as their respective carbon chemical shifts.

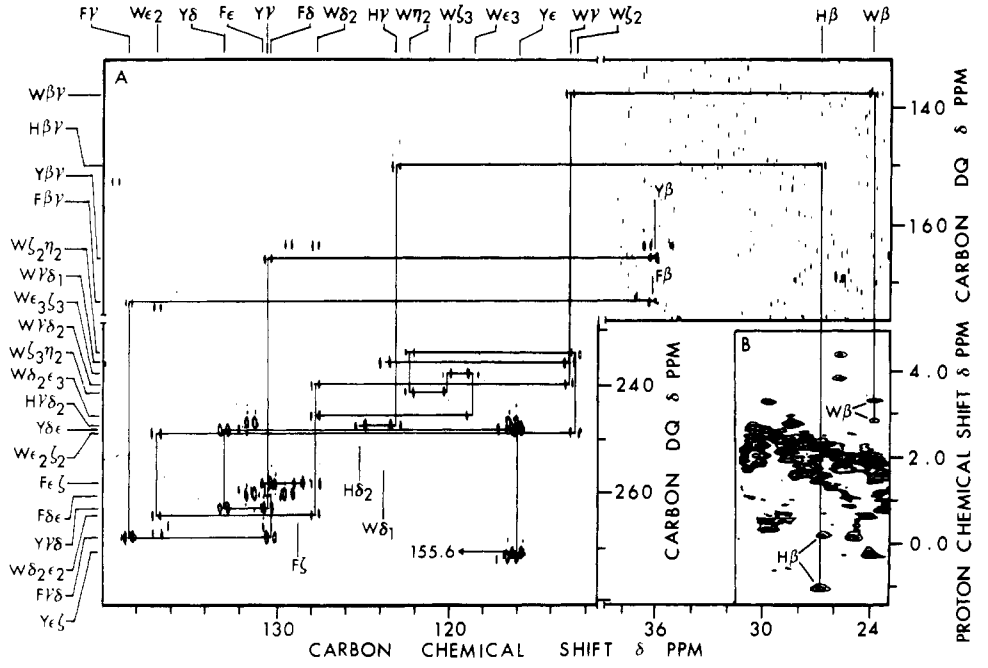

FIGURE 4: Composite 11.7-T NMR spectra of cytochrome *c*-553 showing the proton β, carbon β, and carbon aromatic regions. Peaks are labeled as in Figure 1. Only selected spin systems are outlined; they correspond to the first example of each type of amino acid listed in Table II. The sample was 15 mM [^{13}C]cytochrome *c*-553 (26% uniformly labeled) in ^2H_2O containing 50 mM phosphate buffer at pH 5.6 at 40 °C; the total sample volume was 0.15 mL in a 5-mm (o.d.) cylindrical microcell. (A) Selected regions of the ^{13}C{^{13}C}DQC spectrum. A total of 314 blocks containing the average of 256 free induction decays (8192 data points each) were collected. The 90° carbon pulse was 7 μs. The sweep width used was 25 000 Hz. The total delay for the double-quantum propagator was set to 9.08 ms. The acquisition time was 0.163 s with a relaxation delay of 1.7 s. (B) β region of the ^{1}H{^{13}C}SBC spectrum. A total of 512 blocks each containing the average of 32 free induction decays (4096 data points each) were collected. The 90° proton pulse was 7 μs, while the 90° carbon pulse was 73 μs. The proton sweep width was 7462 Hz, and the carbon sweep width was 8929 Hz (covering only the aliphatic region). The delay time used was 3.57 ms to optimize for 140-Hz carbon–proton couplings. The acquisition time was 0.274 s with a relaxation delay of 1.6 s.

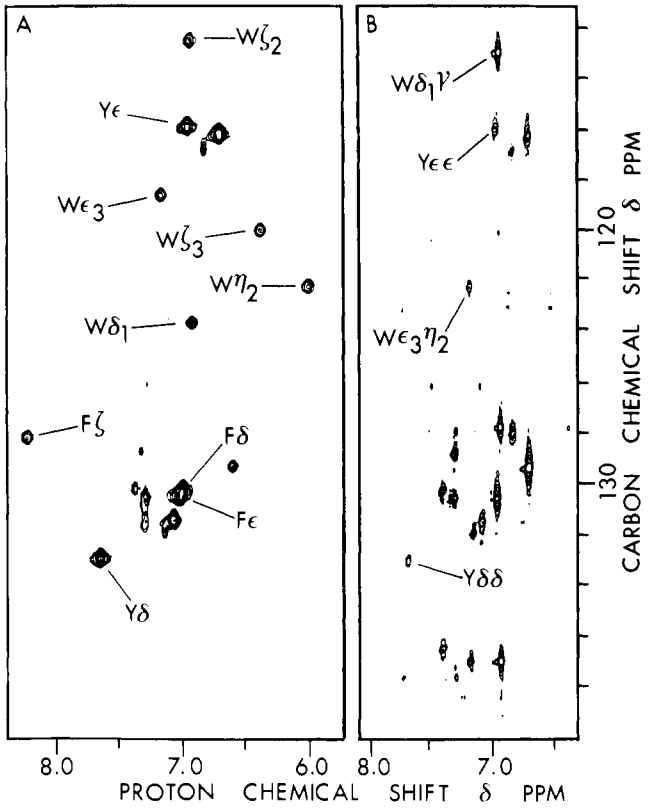

FIGURE 5: Composite 11.7-T NMR spectra of cytochrome *c*-553 showing the aromatic region. Sample conditions were as described in the legend to Figure 4. Each identified cross peak is associated with the outlined spin systems in Figure 4. (A) Region of the ^1H-$\{^{13}C\}$SBC spectrum. Peak notation is *Pr*, where *P* is the single-letter amino acid abbreviation and *r* is the Greek letter identifying the type of carbon and proton atoms involved in the correlation. Experimental parameters were as described in the legend to Figure 4, except that the carbon sweep width was 7172 Hz (covering only the aromatic region) and the delay time used was 2.94 ms to optimize for 170-Hz carbon–proton couplings. (B) Region of the $^1H\{^{13}C\}$MBC spectrum. Peaks are labeled according to the notation *Prs*, where *P* is the single-letter amino acid abbreviation and *r* and *s* are Greek letters identifying the atoms whose resonances along the horizontal and vertical frequency axes, respectively, give rise to the cross peaks. A total of 1024 blocks each containing the average of 32 free induction decays (4096 data points each) were collected. The 90° proton pulse was 7 μs, while the 90° carbon pulse was 8 μs. The proton sweep width was 7462 Hz, and the carbon sweep width was 22 266 Hz. A 2.94-ms delay was used to suppress one-bond couplings. A 70-ms delay was used to optimize for 7-Hz carbon–proton couplings. The acquisition time was 0.274 s with a relaxation delay of 1.6 s.

the β-carbons then can be used to exit the carbon spin system and assign the β-proton resonances. In this way, aromatic ring proton resonances can be correlated with β-proton resonances by utilizing only through-bond connectivities.

Elucidation of intraresidue (^1H, ^{13}C, ^{15}N) spin systems by the methods outlined here can be combined with various sequential assignment strategies: the conventional approach based on interresidue nuclear Overhauser effects (Billeter et al., 1982) or methods based on interresidue heteronuclear scalar coupling (Kainosho & Tsuji, 1982; Kainosho et al., 1987; Westler et al., 1988a,b). Assignment of main-chain carbonyl carbon and amide nitrogen resonances (Figure 3) is required for the heteronuclear scalar coupling strategies. The methods described here are being applied in our laboratory to proteins that have been cloned and overproduced in *Escherichia coli*. This concerted heteronuclear approach to resonance assignments in proteins will enable larger proteins (M_r >20 000) to be subjected to comprehensive NMR analysis.

Table II: Aromatic Proton, Carbon, and Nitrogen Chemical Shifts in *Anabaena* 7120 Flavodoxin and Cytochrome *c*-553

	carbon										proton							nitrogen	
amino acid[a]	β	γ	δ^b	δ_2	ϵ^b	ϵ_2	ϵ_3	ξ	ξ_2	ξ_3	η_2	β	δ^b	ϵ^b	ϵ_3	ξ	ξ_2	ξ_3	η_2	ϵ_1	δ_1, ϵ_2[c]
Flavodoxin																					
His	29.6	126.8		123.5	134.6								5.83	7.78							177.5, 231.5
Tyr-a		128.1	132.0		117.6			156.6					7.13	6.85							
Tyr-b		129.2	130.8		115.4			156.2					7.39	6.79							
Tyr-c		127.7	130.6		115.5			155.2					7.03	6.73							
Trp-a	26.7	108.3	125.3	128.8		136.9	117.4		115.1	117.9	122.3		7.53		6.94		8.25	6.59	6.82	134.0	
Trp-b	32.9	109.8	124.6	127.8		137.4	120.0		113.9	119.3	121.1		7.33		8.01		7.56	6.88	6.92	130.4	
Trp-c	32.0	112.0	119.5	126.2		137.3	116.5		114.0	120.4	122.8		6.40		6.97		8.13	7.09	7.35	131.6	
Trp-d	29.4	112.4	124.3	127.5		137.7	120.1		112.3	119.3	123.4		7.29		8.16		7.61	7.38	7.52	126.3	
Cytochrome *c*-553																					
His[d]	26.5	123.0		125.3	134.0							−1.23, 0.08	0.19	1.30							158.0, 173.4
Phe-a	36.2	138.3	130.4			130.6		128.3					7.05	7.06		8.21					
Phe-b	38.8	136.8	130.6										7.40								
Tyr-a	36.3	130.4	133.1			116.1		155.6					7.66	6.99							
Tyr-b	34.8	129.1	131.5			116.4		156.2					7.10	6.75							
Trp	23.7	113.0	123.8	127.8		136.9	118.8		112.7	120.2	122.4	2.83, 3.33	6.97		7.19		6.98	6.44	6.09	125.0	

[a] Different residues of a given type of amino acid have been assigned a letter here and in the figures. The primary sequence of neither protein has been determined. [b] Chemical shifts of the δ- and ε-carbons (and protons) of each phenylalanine and tyrosine appear to overlap. [c] Individual assignments of the histidine δ_1- and ϵ_2-nitrogens were not determined. [d] Heme iron ligand.

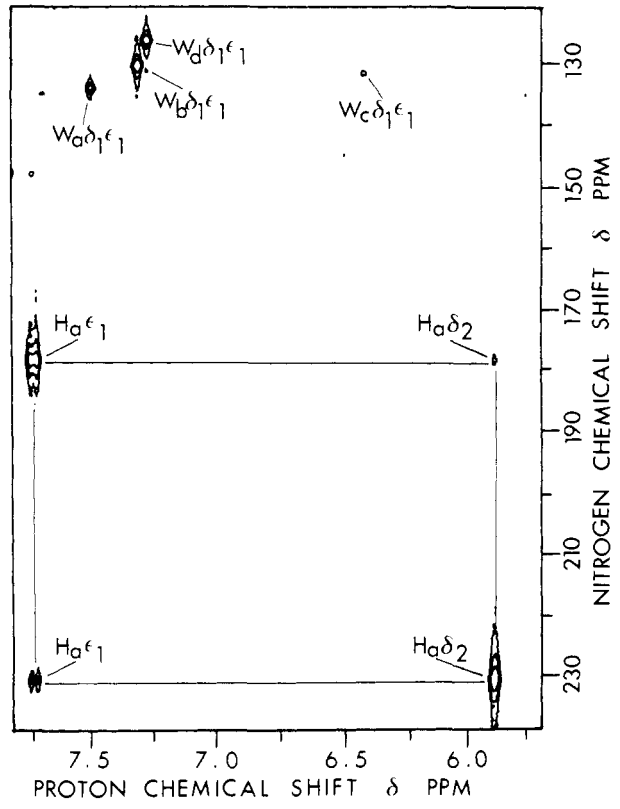

FIGURE 6: Aromatic correlations in the 11.7-T NMR $^1H\{^{15}N\}$MBC spectrum of flavodoxin. Peaks are labeled according to the notation P_qrs, where P is the single-letter amino acid abbreviation, q corresponds to the amino acid lettering in the data tables, and r and s are Greek letters identifying the atoms whose resonances along the horizontal and vertical frequency axes, respectively, give rise to the cross peak. Only the proton chemical shift is given for the histidine correlations. Sample conditions and experimental parameters were as described in the legend to Figure 3.

ACKNOWLEDGMENTS

We thank Dr. David W. Krogmann for the culture of *Anabaena* 7120 and for supplying the flavodoxin isolation procedure prior to publication. We thank Dr. Ed S. Mooberry for optimizing the NMR instrumentation and Denise A. Benway for valuable technical assistance.

Registry No. Cytochrome *c*-553, 12624-01-0.

REFERENCES

Allerhand, A. (1979) *Methods Enzymol. 61*, 458–549.
Bax, A., & Drobny, G. (1985) *J. Magn. Reson. 61*, 306–320.
Bax, A., & Summers, M. L. (1986) *J. Am. Chem. Soc. 108*, 2093–2094.
Bax, A., Griffey, R. H., & Hawkins, B. L. (1983) *J. Magn. Reson. 55*, 301–315.
Billeter, M., Braun, W., & Wüthrich, K. (1982) *J. Mol. Biol. 155*, 321–346.
Brühwiler, D., & Wagner, G. (1986) *J. Magn. Reson. 69*, 546–551.
Bystrov, V. F. (1976) *Prog. Nucl. Magn. Reson. Spectrosc. 10*, 41–81.
Chan, T.-M., & Markley, J. L. (1982) *J. Am. Chem. Soc. 104*, 4010.
Chan, T.-M., & Markley, J. L. (1983) *Biochemistry 22*, 5996–6002.
Dalvit, C., Wright, P. E., & Rance, M. (1987) *J. Magn. Reson. 71*, 539–543.
Davis, D. G., & Bax, A. (1985) *J. Am. Chem. Soc. 107*, 2820–2821.
Glushka, J., & Cowburn, D. (1987) *J. Am. Chem. Soc. 109*, 7879–7881.
Griffey, R. H., & Redfield, A. G. (1987) *Q. Rev. Biophys. 19*, 51–82.
Griffey, R. H., Jarema, M. A., Kunz, S., Rosemear, P. R., & Redfield, A. G. (1985) *J. Am. Chem. Soc. 107*, 711–712.
Jardetzky, O. (1981) *Acc. Chem. Res. 14*, 291–298.
Kainosho, M., & Tsuji, T. (1982) *Biochemistry 21*, 6273–6279.
Kainosho, M., Nagao, H., & Tsuji, T. (1987) *Biochemistry 26*, 1068–1075.
Karplus, S., & Karplus, M. (1972) *Proc. Natl. Acad. Sci. U.S.A. 69*, 3204–3206.
Kojiro, C. L., & Markley, J. L. (1983) *FEBS Lett. 162*, 52–56.
Kumar, A., Ernst, R. R., & Wüthrich, K. (1980) *Biochem. Biophys. Res. Commun. 95*, 1–6.
Levitt, M. H., & Ernst, R. R. (1983) *Mol. Phys. 50*, 1109–1124.
McCain, D. C., Ulrich, E. L., & Markley, J. L. (1988) *J. Magn. Reson.* (in press).
McIntosh, L. P., Griffey, R. H., Muchmore, D. C., Nielson, C. P., Redfield, A. G., & Dahlquist, F. W. (1987) *Proc. Natl. Acad. Sci. U.S.A. 84*, 1244–1248.
Nagayama, K., Kumar, A., Wüthrich, K., & Ernst, R. R. (1980) *J. Magn. Reson. 40*, 321–334.
Oh, B. H., Westler, W. M., Darba, P., & Markley, J. L. (1988) *Science (Washington, D.C.) 240*, 908–911.
Ortiz-Polo, G., Krishnamoorthi, R., Markley, J. L., Live, D. H., Davis, D. G., & Cowburn, D. (1986) *J. Magn. Reson. 68*, 303–310.
Rance, M., Wright, P. E., Messerle, B. A., & Field, L. D. (1987) *J. Am. Chem. Soc. 109*, 1591–1593.
Richarz, R., & Wüthrich, K. (1978) *Biopolymers 17*, 2133–2141.
Senn, H., Otting, G., & Wüthrich, K. (1987) *J. Am. Chem. Soc. 109*, 1090–1092.
Shaka, A. J., Keeler, J., Frenkiel, T., & Freeman, R. (1983) *J. Magn. Reson. 52*, 335–338.
Sklenar, V., & Bax, A. (1987) *J. Magn. Reson. 71*, 379–383.
Smith, G. M., Liping, P. Y., & Domingues, D. J. (1987) *Biochemistry 26*, 2202–2207.
Stockman, B. J., Westler, W. M., Mooberry, E. S., & Markley, J. L. (1988a) *Biochemistry 27*, 136–142.
Stockman, B. J., Westler, W. M., Darba, P., & Markley, J. L. (1988b) *J. Am. Chem. Soc. 110*, 4095–4096.
Ulrich, E. L. (1978) Ph.D. Thesis, Purdue University.
Westler, W. M., Kainosho, M., Nagao, H., Tomonaga, N., & Markley, J. L. (1988a) *J. Am. Chem. Soc. 110*, 4093–4095.
Westler, W. M., Stockman, B. J., Hosoya, Y., Miyake, Y., Kainosho, M., & Markley, J. L. (1988b) *J. Am. Chem. Soc. 110*, 6256–6258.
Wüthrich, K. (1986) *NMR of Proteins and Nucleic Acids*, pp 1–292, Wiley, New York.
Wüthrich, K., Wider, G., Wagner, G., & Braun, W. (1982) *J. Mol. Biol. 155*, 311–319.